

International Conference on Space Optics—ICSO 2018

Chania, Greece

9–12 October 2018

Edited by Zoran Sodnik, Nikos Karafolas, and Bruno Cugny



Teledyne's high performance infrared detectors for Space missions

Paul Jerram

James Beletic



icso proceedings



International Conference on Space Optics — ICSO 2018, edited by Zoran Sodnik, Nikos Karafolas, Bruno Cugny, Proc. of SPIE Vol. 11180, 111803D · © 2018 ESA and CNES · CCC code: 0277-786X/18/\$18 · doi: 10.1117/12.2536040

Teledyne's High Performance Infrared Detectors for Space Missions

Paul Jerram^a and James Beletic^b

^aTeledyne e2v Space Imaging, Chelmsford, UK, CM7 4BS

^bTeledyne Imaging Sensors, Camarillo, California, USA 93012

ABSTRACT

Teledyne is one of the world's leaders in the provision of infrared sensors for Earth science, planetary science, and astronomy. This paper presents Teledyne's focal plane array technologies that provide high performance for space missions, with sections on substrate-removed HgCdTe (*that provides simultaneous visible / IR detection*) and fully depleted HgCdTe (*that enables detectors to be operated at significantly increased temperatures*). We give examples of the image sensors provided for Euclid, WFIRST, AVIRIS-NG, ECOSTRESS, and NEOCam.

Keywords: Mercury Cadmium Telluride, HgCdTe, Infrared

1. INTRODUCTION

Mercury Cadmium Telluride (HgCdTe or MCT) is used in applications where the highest performance IR detectors are required. HgCdTe achieves the highest quantum efficiency and lowest dark current of any IR detector material, and the cutoff wavelength of HgCdTe can be tuned over a wide range of wavelengths from NIR to LWIR.

HgCdTe is a II-VI detector material with 50% of the atoms (Hg, Cd) from column II of the period table of elements and 50% of the atoms (Te) from column VI. The bandgap of HgCdTe is tuned by adjusting the ratio of mercury to cadmium as described by the equation published by Hansen et al (1); see Fig. 1. Note that for smaller bandgaps (longer cutoff wavelengths) there is a strong temperature dependence which must be taken into account when fabricating the detectors.

$$E_g = -0.302x + 1.93x^2 + 0.832x^3 + 5.35 \times 10^{-4} T (1-2x)$$

Where E_g is the bandgap of the material in electron volts (eV), x is the cadmium mole fraction, and T is temperature in deg K.

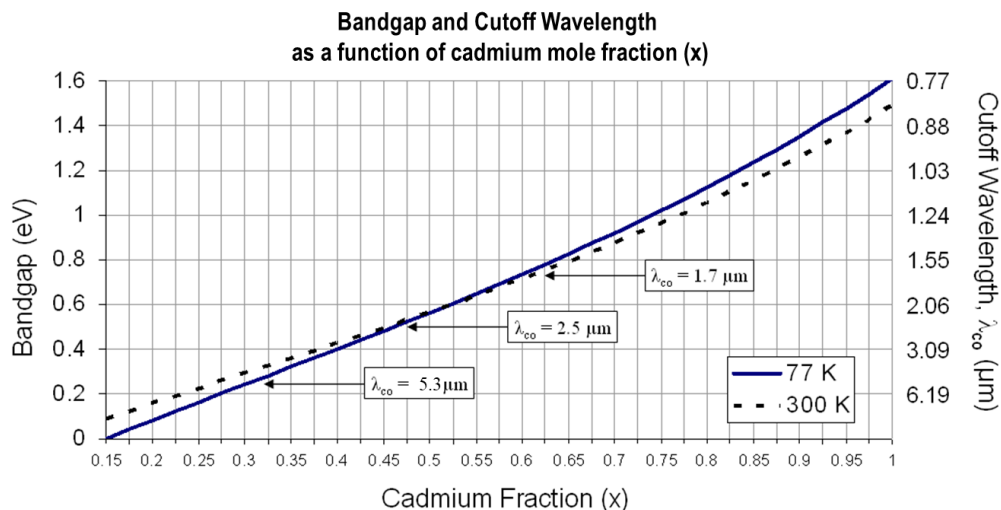


Figure 1: Bandgap and cutoff wavelength of $Hg_{(1-x)}Cd_xTe$ as a function of cadmium fraction x

Teledyne's HgCdTe architecture is p-on-n, which means that the signal collected at the readout circuit are holes (the absence of electrons) and the photoelectrons are conducted to the back surface of the detector and connected to a

substrate bias voltage. The basic structure of a hybrid IR focal plane array is shown in Fig. 2. The HgCdTe material is grown at Teledyne after which it is processed to form an array of photodiodes that are bump bonded to pixels in the Readout Integrated Circuit (ROIC). The HgCdTe photodiode array and the ROIC are separately optimized and a given ROIC can be hybridized to several types of detector materials (e.g. HgCdTe, Si, InGaAs).

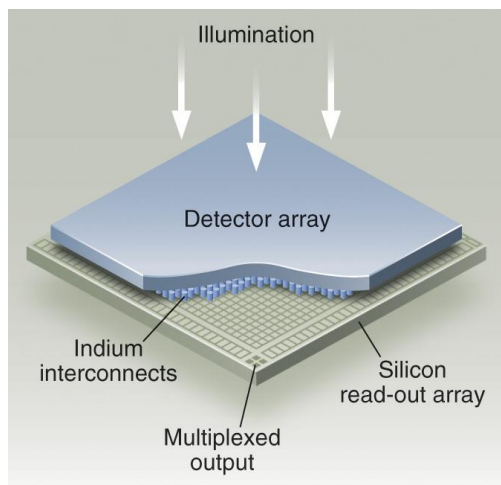


Figure 2: Hybrid CMOS FPA architecture

The composition of the HgCdTe detector array determines the operating wavelength range, the quantum efficiency (QE), the dark signal and the radiation performance

The silicon read-out array defines the readout noise, peak signal, frame rate or cadence, operating modes including windowing, interfaces, radiation performance, linearity and anti-blooming performance

The interconnect process is critical in determining the operability or percentage of fully functioning pixels

In order to obtain the highest performance focal plane arrays, three aspects of the technology must be optimized: (1) growth and processing of the detector material, (2) design and fabrication of the ROIC, and (3) hybridization of the detector array to the ROIC and subsequent detector processing. This paper will present some aspects of Teledyne's FPA fabrication process and will give examples of sensors that have been developed using this technology.

2. TECHNOLOGY DEVELOPMENT

2.1 Mercury Cadmium Telluride Detector growth and processing

The manufacturing method that produces the highest performance HgCdTe material is molecular beam epitaxy (MBE) with a double-layer planar hetero-junction (DLPH) detector architecture. An MBE machine grows the HgCdTe layer on a CdZnTe substrate with a cadmium fraction that determines the bandgap as described in the previous section. CdZnTe has a lattice spacing of ~ 0.64 nm which is nearly identical to that of HgCdTe which enables HgCdTe on CdZnTe to be produced with a very pure, low defect, crystalline structure. The HgCdTe is deposited one atomic layer at a time taking about 6 hours to grow a complete detector layer. The mixture of Hg, Cd, and Te is monitored as the atomic layers are deposited using spectroscopic reflectance ellipsometry, which gives highly accurate measurements of the HgCdTe structure during deposition and enables precise control of the bandgap structure which is varied during material growth.

When the detector is hybridized to the ROIC, the CdZnTe substrate is on the side of the detector facing the incident illumination. Since CdZnTe is opaque to wavelengths shorter than 900 nm, a "substrate on" detector is insensitive to visible light.

Substrate removed technology: Teledyne has developed a process for removal of the CdZnTe substrate material and substrate removal is now standard for all NIR, SWIR and MWIR focal plane arrays made by Teledyne. Substrate removal involves taking off all of the CdZnTe substrate after hybridization to leave a layer of HgCdTe that is only 7 to 10 μm thick. After substrate removal an anti-reflection (AR) is deposited on the HgCdTe. Substrate removal has a number of significant advantages, including:

- Sensitivity to visible light, down to 380 nm, with a significant increase in quantum efficiency below 1.3 μm .

- Elimination of fluorescence from cosmic rays absorbed in the CdZnTe substrate – very important for low light level space applications
- Elimination of Fabry-Perot fringes that can occur in the substrate with narrow band illumination, such as in spectrometers

Fig. 3 shows the improvement in QE that is obtained with a substrate removed detector with a cutoff wavelength of 1.7 μm and an optimized multi-layer AR coating.

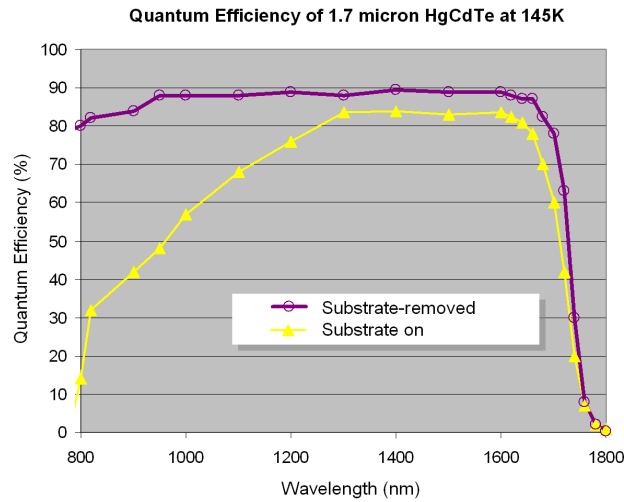


Figure 3: Quantum Efficiency of a substrate removed HgCdTe detector with 1.7 μm cutoff

Dark Current: Quantum efficiency, dark current, and readout noise are the three most important parameters that describe high performance detectors. Dark current, which is the charge collected by a detector in the absence of light, cannot be distinguished from photo-generated charge and low signal applications such as astronomy require very low levels of dark current. HgCdTe detectors grown by MBE achieve the lowest dark current, which is often described by an empirically derived formula called Rule 07 (see Fig. 4).

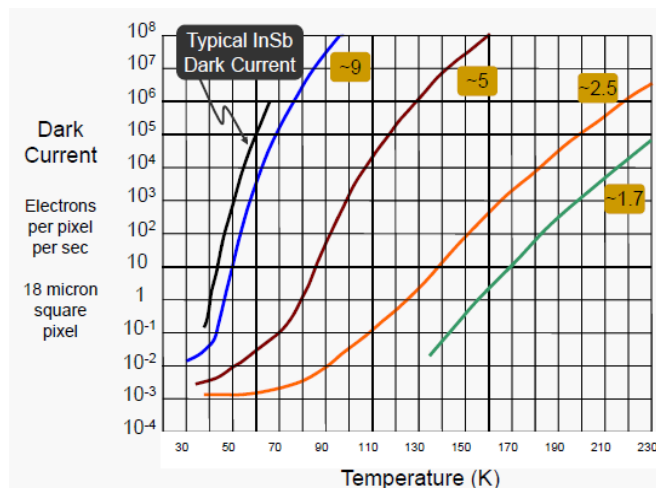


Figure 4: Dark current for Teledyne detectors as a function of temperature and cutoff wavelength

For NIR and SWIR HgCdTe (1.7 and 2.5 μm cutoff), the main cause of dark current are defects in the crystal lattice. For MWIR, LWIR, and VLWIR detectors ($\lambda_{\text{co}} = 5.3, 10, \text{ and } 14.5 \mu\text{m}$) the main cause of dark current is the thermal energy of free electrons in the non-depleted volume of the detector. When the thermal energy of these free electrons are absorbed by the crystal lattice, electrons can be released which creates dark current. This is called the Auger-1 process, which is the dominant source of dark current in high quality MWIR, LWIR, and VLWIR HgCdTe detectors below 130K and 100K respectively.

Fully depleted HgCdTe: Teledyne has developed a process to fabricate lightly doped HgCdTe detectors that can be fully depleted with minimal (1-2 volt) reverse bias (2). A fully depleted detector has removed most of the free electrons which suppresses the Auger-1 dark current signal to the point where “dark current” is dominated by the radiative background seen by the detector. Depending on cutoff wavelength and operating temperature, the radiative background is a factor of 10 to 100 lower than Rule07 (Auger-1) dark current. This gives a major advantage for space applications, enabling operation at a much higher temperature with passive cooling or smaller cryo-coolers. Figure 5 shows the increase in operating temperature that can be obtained with the use of fully depleted HgCdTe detectors.

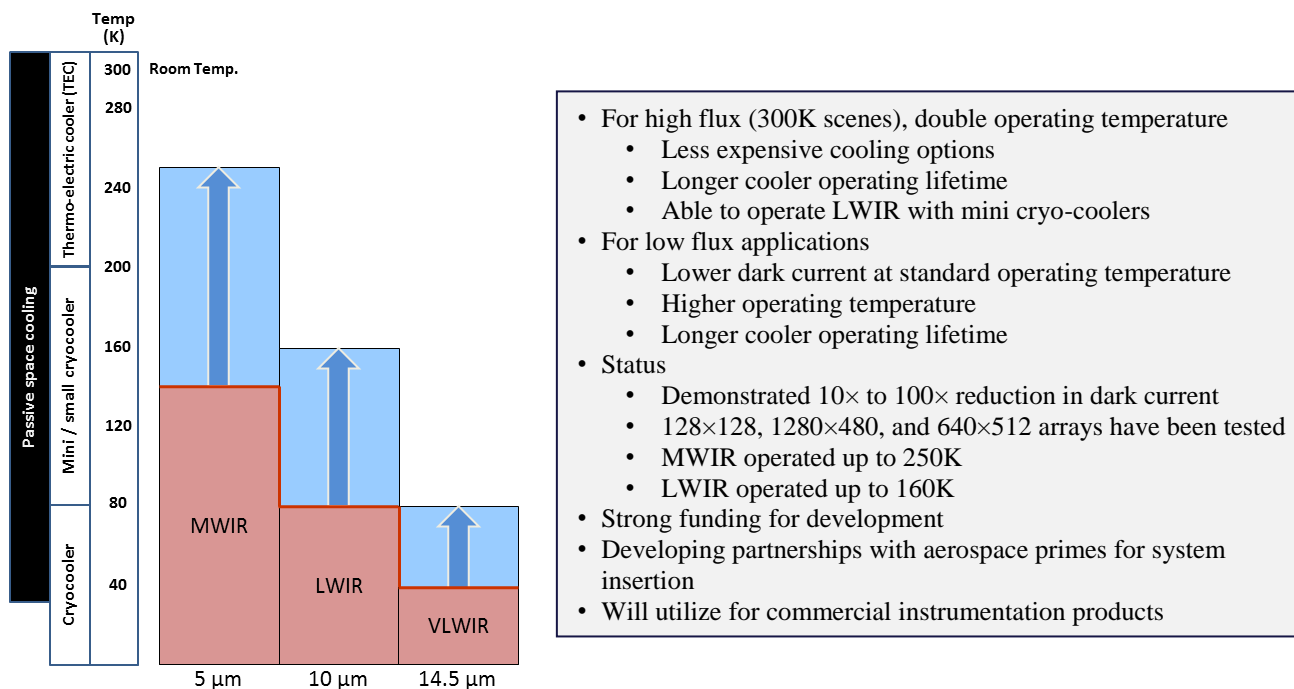


Figure 5: Increase in operating temperature from the use of fully depleted HgCdTe

2.2 ROIC technology developments

ROICs have been developed for Earth observation and planetary observation applications that have flexible formats. The CHROMA ROIC which is optimized for spectrometers (hyperspectral imaging) has 30 μm square pixels, a capacitive transimpedance amplifier (CTIA), and has been produced in four different formats: 320 \times 480, 640 \times 480, 1280 \times 480, and 1600 \times 480 pixels. There is a single full well in each pixel which can be optimized for the application; full wells that have been produced include 700 ke-, 1Me-, and 5 Me-. CHROMA has been used by the Jet Propulsion Laboratory (JPL) in a number of spectrometers including AVIRIS-NG, NEON, PRISM, and Europa MISE. Table 1 presents information on the CHROMA formats that are available. For full frame readout (480 rows), the maximum frame rate is 125 Hz. CHROMA has an analogue output every 160 columns and operates in integrate-while-read mode.

Table 1: CHROMA ROIC configurations

Array Format	Well capacity & Readout Noise			Power dissipation at 125 Hz [mW]	ROIC dimensions [mm]	No. Outputs
	CDS Noise Well = 0.7M e-	CDS Noise Well = 1M e-	CDS Noise Well = 5M e-			
CHROMA-320	120 e-	145 e-	600 e-	70	14.4 x 19.4	2
CHROMA-640	120 e-	145 e-	600 e-	90	24.4 x 19.5	4
CHROMA-1280	120 e-	145 e-	600 e-	150	43.2 x 19.6	8
CHROMA-1600	120 e-	145 e-	600 e-	180	52.8 x 19.7	10

The most recent ROIC development at Teledyne has been the CHROMA-D / GeoSnap ROIC. This is a highly flexible stitched format that can be fabricated in a number of different formats. The ROIC stitch blocks are shown in the left side of Fig. 6. Stitching is a well-established fabrication process for making large imaging sensors.

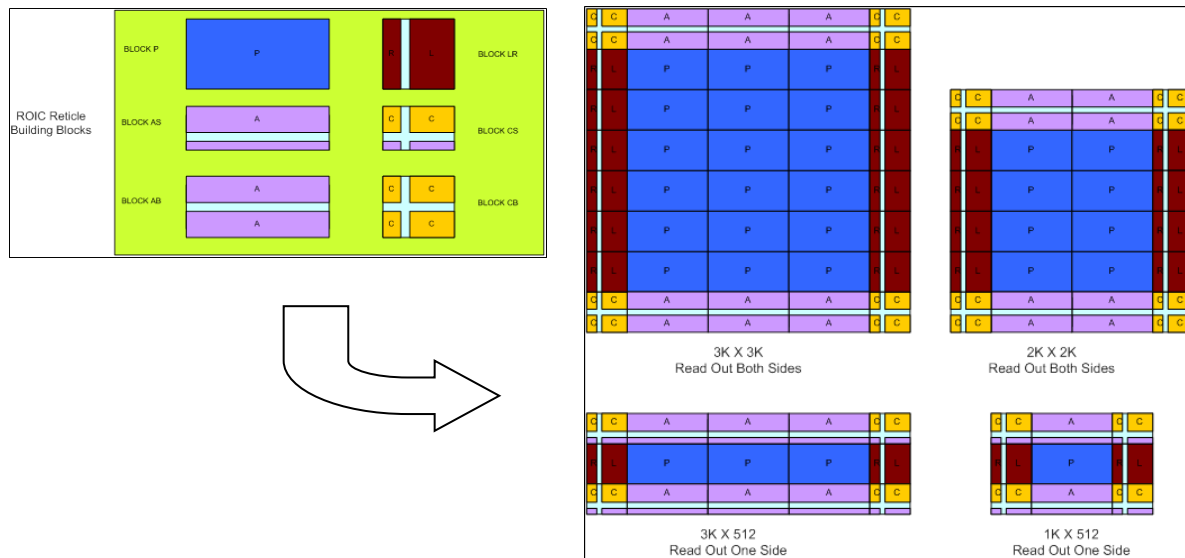


Figure 6: GeoSnap / CHROMA-D mask set and examples of formats that can be manufactured

The pixel stitch block (P, shown in blue) is 512 rows by 1024 columns of 18 μm square pixels. The largest ROIC that can be made with this design stitches together 18 pixel blocks to produce a 3K \times 3K array. The CHROMA-D ROIC has digital input and digital output greatly easing the interface to external electronics. This ROIC has a CTIA pixel cell with two gains (row programmable) and 14 bit column parallel ADCs. To date, the GeoSnap / CHROMA-D array has been manufactured in 2K \times 2K, 2K \times 512, and 3K \times 512 formats. The maximum frame rate depends on whether there are outputs only at the bottom edge or along both the top and bottom, and the number of rows read out. Frame rate is independent of width. For the 2K \times 512 and 3K \times 512 formats with outputs on the bottom side, the maximum full frame (512 rows) rate is 250 Hz.

3. EXAMPLES OF DEVICES USED FOR SPACE APPLICATIONS

3.1 Astronomy applications

The HxRG family of detectors are the most widely used detector in ground-based and space astronomy instrumentation. Most space missions and ground-based observatories have used the 1K \times 1K format (H1RG) or 2K \times 2K format (H2RG) 18 μm pixel pitch arrays that have been available for over 15 years. The newest generation HxRG arrays are the 16 million pixel H4RG arrays, that are made in 10 μm (H4RG-10) and 15 μm (H4RG-15) pixel pitch. The H4RG-15,

which at 6×6 cm size is the largest format high performance astronomy array available, is now a mature product, having been delivered to instruments at five observatories and operating on a nightly basis at telescopes in Hawai'i. The European Southern Observatory will received four H4RG-15 arrays for the MOONS instrument of ESO's Very Large Telescope and 15 H4RG-15 arrays for use in the MICADO and HARMONI instruments of ESO's Extremely Large Telescope.

3.2 ESA Euclid dark energy mission

The H2RG devices produced for Euclid are a good example of the performance achieved by the HxRG arrays. Euclid will use 16 H2RG arrays with accompanying SIDECAR ASIC modules as shown in Fig. 7. When Euclid launches in 2021, it will be the largest IR focal plane operating in space (67 million pixels). The H2RG arrays have been delivered to ESA after testing at the Goddard Space Flight Center Detector Characterization Laboratory. (*NASA is a partner with ESA in Euclid, providing the IR arrays and SIDECAR ASIC focal plane electronics*). Figure 7 shows the quantum efficiency measured for the 24 flight candidate arrays that Teledyne delivered to NASA; the measured QE greatly exceeds the 74% specification set by Euclid. The dark current and readout noise of all 24 flight candidate arrays are also much better than required by the specification, as shown in Fig. 8.

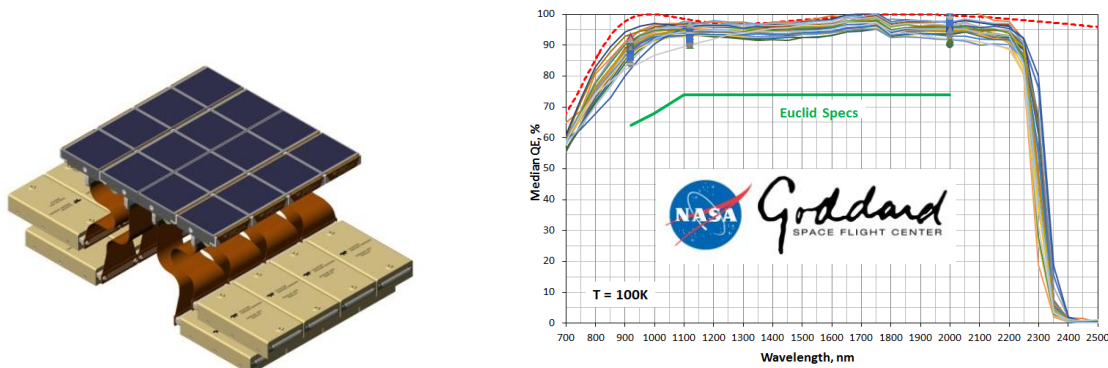


Figure 7: The Euclid focal plane assembly with 16 H2RG arrays and 16 SIDECAR ASIC modules (left) and quantum efficiency of 24 flight candidate arrays measured by Goddard's Detector Characterization Laboratory (right)

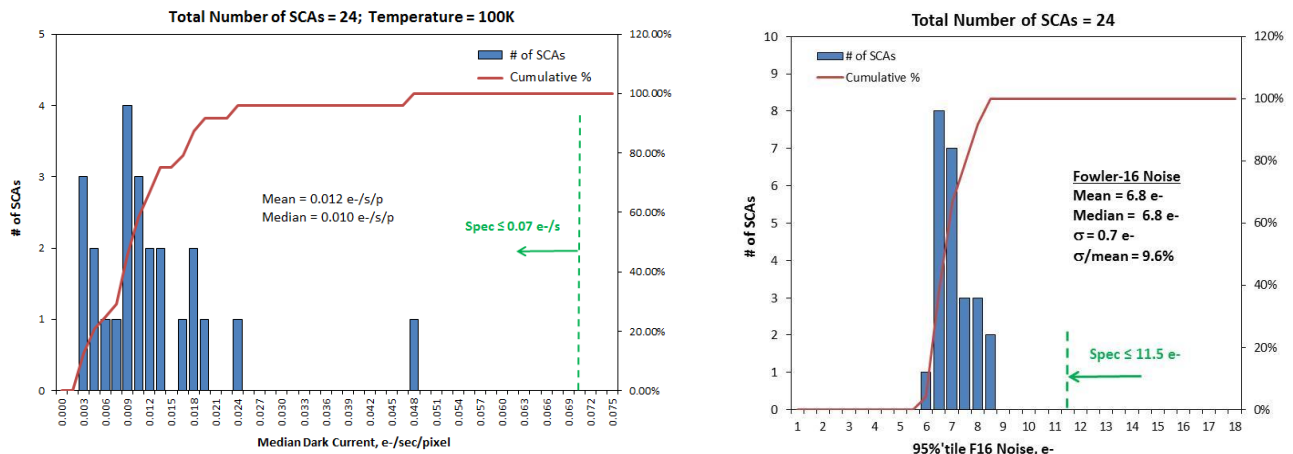


Figure 8: Dark current and readout noise measured at Teledyne for 24 Euclid flight candidate H2RG arrays

3.3 NASA WFIRST

NASA's Wide Field Infrared Survey Telescope (WFIRST) is NASA's next flagship astronomy mission after JWST. WFIRST will have the largest IR focal plane array operating in space when it launches in the mid 2020's; more than 300 million pixels composed of eighteen (18) H4RG-10 arrays. During 2014-2018, NASA conducted a four year development program for the H4RG-15 SWIR (2.5 μm cutoff) array to improve performance in several ways including hybridization (achieving 99.99% interconnect operability), and reduction of readout noise and image persistence. The WFIRST development program achieved all performance specifications and demonstrated the yield required for the flight mission. Production of the flight arrays commenced in June 2018 and will conclude by the end of 2020.

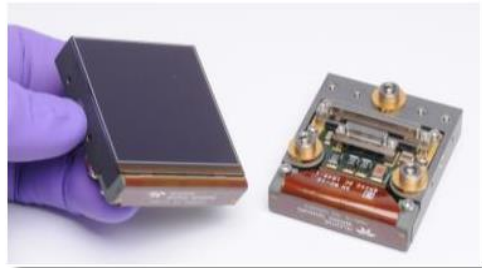


Figure 9: The H4RG-10, 4K \times 4K pixels, 10 μm pixel pitch

3.4 AVIRIS-NG

The Airborne Visible Infra-Red Imaging Spectrometer – Next Generation (AVIRIS-NG) instrument was developed by the Jet Propulsion Laboratory (JPL) for airborne observations that are conducted worldwide, with the most recent campaign conducted during June 2018 in the European Alps. The Offner spectrometer (Fig. 10 left) uses a CHROMA 640 \times 480 pixel substrate-removed Vis-SWIR (380-2530 nm) array to study the biology and geology of the Earth's surface using reflected sunlight spectroscopy. An example of a data cube from AVIRIS-NG is shown in Fig. 10 (right).

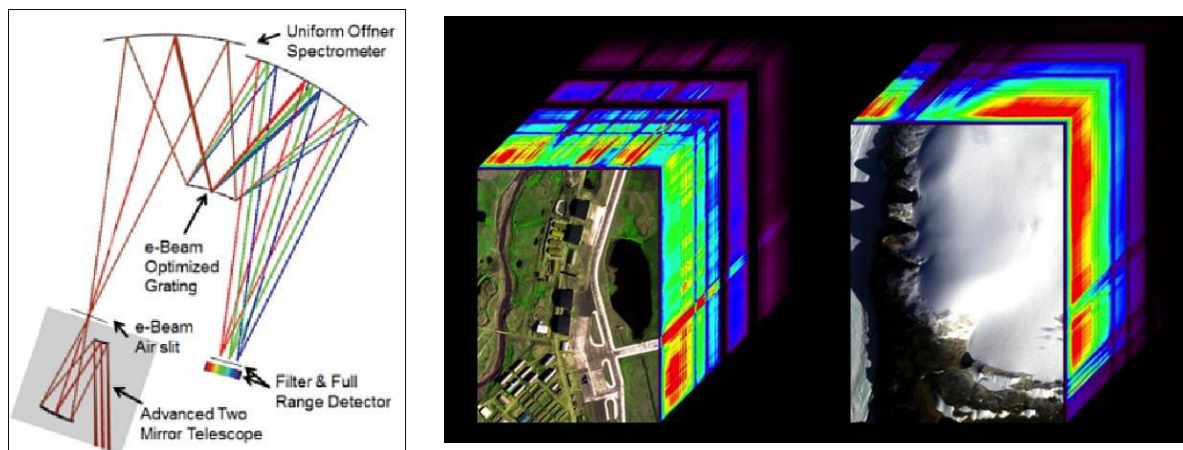


Figure 10: AVIRIS-NG spectrometer optical design (left) and example data cubes (right). Courtesy JPL.

3.5 ECOSTRESS

ECOSTRESS (ECOSystem Spaceborne Thermal Radiometer Experiment on Space Station) is a multispectral instrument operating in MWIR and LWIR bands with wavelengths from 4 to 12 μm . This JPL instrument, which was successfully commissioned on the ISS in July 2018, operates in whiskbroom mode, rapidly scanning across the Earth in a direction orthogonal to the spacecraft orbit. To do this, the multi-spectral array must read out at 30,000 frames per second, reading 4 rows of pixels per color to achieve 100% pixel operability per band. The ECOSTRESS ROIC is an array of 8 bands,

each with 32 rows of 256 pixels, with 40 μm pixel pitch. This is a digital input, analogue output array, with 32 high speed ports. At the operating temperature of 60 K, the dark signal is 183e-/pixel/sec which is negligible at the operating frame rate. Each of the channels has a different full well capacity optimized to match the expected peak signal in each band. The format of the ECOSTRESS FPA device is shown in Fig. 11. The first images from the sensor operating on the International Space Station can be found on the NASA JPL website: <https://ecostress.jpl.nasa.gov/>

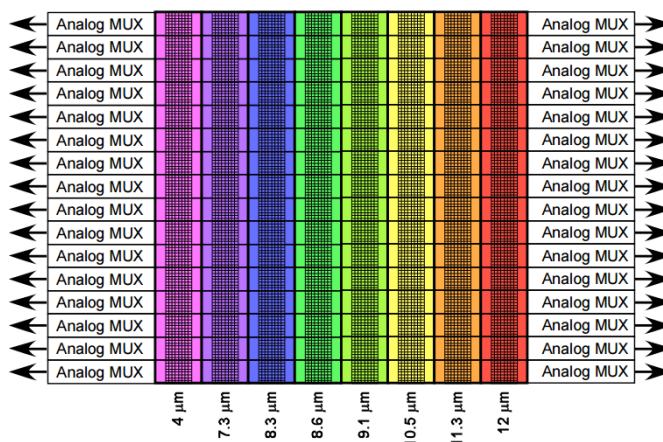


Figure 11: ECOSTRESS focal plane array configuration

3.6 NEOCam Asteroid Survey Mission

The Near Earth Object Camera (NEOCam) asteroid survey mission will discover and characterise the largest and most potentially hazardous asteroids that have orbits that bring them near the Earth. NEOCam is currently in an Extended Phase A during which the infrared detectors are being optimized in anticipation of future mission selection. The NEOCam instrument will image a 2K \times 8K pixel area of the sky in two bands: MWIR (3-5 μm) and LWIR (6-10 μm). Simultaneously measuring MWIR and LWIR emission will enable NEOCam to accurately measure the size of the asteroids. Teledyne has been working with JPL for nearly 8 years to develop and demonstrate the IR detectors that are required for NEOCam to be feasible. An important milestone for NEOCam has been the demonstration of high quality 4 megapixel (H2RG) LWIR arrays, the largest high performance LWIR arrays made for low light level astronomy. NEOCam can now proceed with two focal plane assemblies, each with four H2RG arrays for MWIR and LWIR detection. The NEOCam LWIR detector target performance is presented in Table 2:

Table 2: NEOCam LWIR detector specification

Image sensor requirements	
Wavelength (μm)	6-10
Operating temperature range (K)	35-40
Integration time (sec)	10
Dark Current (e-/pixel/sec)	<200
Read noise (Correlated double sample; e-)	<30
Quantum Efficiency (%)	>60
Well depth (e-)	>45 k
Pixel Operability (%) (with all above properties)	>90
(Target)	>95
Focal plane assembly size (pixels)	2K \times 8K

The main challenge for NEOCam is to achieve good operability from a large area LWIR sensor at the required operating temperature. In this case, operability is dominated by the requirement for the dark current to be less than 200 e-/pixel/sec (at that level, the dark current is less than the LWIR background from the zodiacal light). Teledyne has produced LWIR detectors that achieve the target specification with an operability of better than 95% (4). A typical curve showing cumulative dark signal at a temperature of 35K is shown in Fig. 12.

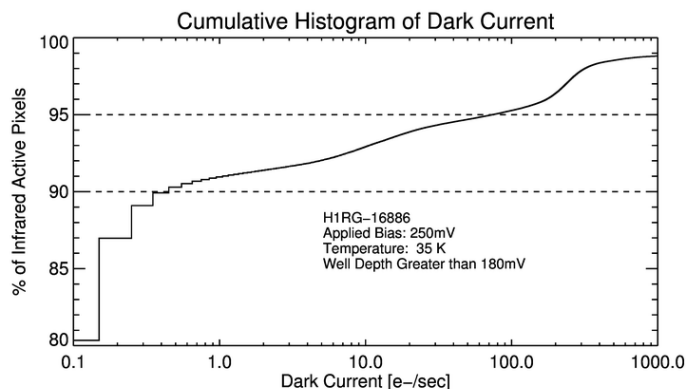


Figure 12: Cumulative dark signal histogram for LWIR H1RG detector for NEOCam

4. SUMMARY

HgCdTe technology remains the infrared detector of choice for space applications for which performance is critical. Teledyne has a proven track record for making high performance HgCdTe and a unique capability to produce the largest format arrays. Recent developments in HgCdTe technology continue to increase the sizes of the arrays and new ROICs provide increased capabilities with digital I/O that provides a much simpler user interface.

The capability of Teledyne to produce large infrared arrays has enabled a number of space astronomy missions that are currently under development including Euclid, WFIRST, and JWST.

REFERENCES

- [1] Hansen, G.L, Schmidt, J.L and Casselman, T.N, "Energy gap versus alloy composition and temperature in $Hg_{1-x}Cd_xTe$ ", J. Appl. Phys. 53(10), 1982, p. 7099.
- [2] Lee, D et al High-Operating Temperature HgCdTe: A Vision for the Near Future. Journal of Electronic Materials. 45. 10.1007/s11664-016-4566-6.
- [3] JPL AVIRIS-NG home page, <https://aviris-ng.jpl.nasa.gov/index.html>
- [4] McMurty, C et al, "Development of sensitive long-wave infrared detector arrays for passively cooled space missions", SPIE Optical Engineering 52(9), September 2013, 091804.
- [5] Beletic, J.W. et al "Teledyne Image Sensors; Infrared imaging technologies for Astronomy and Civil Space", Proc. SPIE 7021, High Energy, Optical, and Infrared Detectors for Astronomy III, 70210H (22 July 2008).